Efficient Coupled Electromagnetic-Thermal Induction Machine Model using scaled FE-Solutions

Martin Nell, Benedikt Groschup and Kay Hameyer
Institute of Electrical Machines (IEM)
RWTH Aachen University
Aachen, Germany
martin.nell@iem.rwth-aachen.de

***Abstract*—Coupled electromagnetic-thermal models are beneficial to simulate the thermal, electromagnetic loss-dependent behavior of machines. Coupling detailed thermal network models and electromagnetic finite element simulation results in high computation time. In this paper a scaling procedure is used to scale the solutions of a in beforehand simulated finite element solution coupled to an analytic three node thermal network model. This approach enables an efficient calculation of the machine temperature considering temperature dependent losses.**

***Index Terms*—induction machine, thermal model, scaling laws, finite element simulation**

I. Introduction

Since the heating of an induction machine (IM) depends on the electromagnetic losses the magnetic and the thermal analysis have to be coupled in the design process [1]. In [2] an analytic thermal network model is coupled to an finite-element (FE)-simulation, where the electric conductivities are updated. In [3] a thermal network model is coupled with an electromagnetic model in the stator reference frame based on the flux-linkage equations and the two axis theory. In [1] an analytic thermal and electromagnetic model, which is parametrized by FE-simulation data, is used to realize the thermal-electromagnetic coupling. In this paper an analytic three node thermal network model is coupled with a scaling procedure enabling a rapid calculation using FE-simulation data. This scaling procedure allows the possibility to scale the solutions, particularly the losses, of a beforehand performed FE-simulation.

II. Thermal Model of the Induction Machine

To simulate the thermal behavior of an IM the thermal three node network model in Fig. 1 is used, which inputs are the FE calculated rotor losses $P_{\mathrm{L,r}}$, the stator ohmic losses $P_{\mathrm{L,ohm,s}}$ and the stator iron losses $P_{\mathrm{L,Fe,s}}$. Node one presents the rotor including the shaft, rotor cage and bearings, node two the stator winding and node three the stator lamination including the housing of the machine.

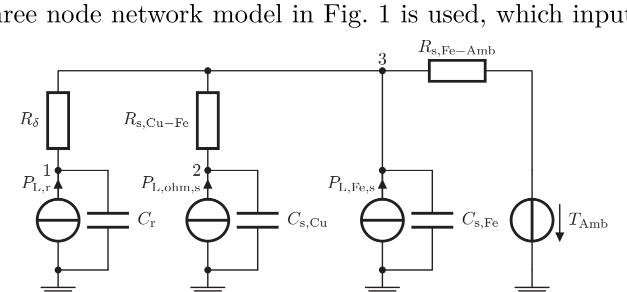

Figure 1: Thermal Three Node Model of the IM.

For the parametrization of the thermal model analytic calculations and an Evolutionary Strategy as described in [4] are applied. The thermal air gap resistance R_δ is calculated according to the approach in [5]. The heat capacity of the stator winding $C_{\mathrm{s,Cu}}$ is calculated by using the mass of the copper winding and its specific thermal capacity. For the heat transfer coefficient from the winding to the stator iron $\alpha_{\mathrm{s,Cu-Fe}}$ and from the stator iron to the ambient $\alpha_{\mathrm{s,Fe-Amb}}$ lower and upper limits, shown in table I, according to [5] and [6] are used. The lower and upper limits of the heat capacity of the rotor C_{r} results from a calculation with a tolerance of $\pm 10\,\%$ of the calculated data. The lower limit of the heat capacity of the stator iron $C_{\mathrm{s,Fe}}$ is calculated by considering only the stator lamination and the upper limit by considering the stator lamination, the housing and the bearing shields. The optimization is carried out on the basis of four measurements and the measured temperatures after 30 min. The torque and speed as well as the measured winding and rotor cage temperature are listed in table II for various operation points. The resulting rotor and winding temperature of the optimization are also listed in table II and show a sufficiently accurate result for the calculations presented here. The resulting data of the parameterization are listed in table I.

Table I: Boundary conditions and results of parameter identification.

Variable	Unit	Lower Limit	Upper Limit	Calculated Data
C_{r}	kJ/K	5.51	6.73	6.71
$C_{\mathrm{s,Fe}}$	kJ/K	11.78	13.6	13.2
$\alpha_{\mathrm{s,Fe-Amb}}$	W/(m^2 K)	25	250	60.94
$\alpha_{\mathrm{s,Cu-Fe}}$	W/(m^2 K)	10	100	74.75

Table II: Derivation of temperatures in measurement and simulation.

#	Speed	Torque	Measurement		Simulation	
			Rotor	Winding	Rotor	Winding
1.	1900 min^{-1}	60 N m	136,7 °C	113 °C	144,6 °C	116,0 °C
2.	3700 min^{-1}	60 N m	171,5 °C	135 °C	181,2 °C	133,8 °C
3.	5700 min^{-1}	37 N m	174,6 °C	135 °C	170,3 °C	133,5 °C
4.	7500 min^{-1}	26 N m	171,8 °C	135 °C	165,5 °C	136,7 °C

III. Scaling Laws of Induction Machines

In [7] an approach to scale the FE solutions of IMs considering geometric variations as well as variations in temperature is proposed. This scaling approach is used in this paper to show the influence of temperature variations in the simulation of IMs.

A. Temperature Scaling of the Stator Resistance

The stator resistance is evaluated in the post processing routine of an IM FE simulation. Therefore, temperature changes in the stator winding can be considered by recalculating the stator resistance R_s using (1). Here, α is the temperature coefficient of the stator winding material, $\vartheta_\mathrm{sim,new}$ the new simulated stator temperature and ϑ_ref the reference temperature. The scaled stator resistance $R_\mathrm{s}^{'}$ leads to scaled Ohmic losses of the stator $P_\mathrm{L,ohm,s}^{'}$ in (2) that are used in the thermal model of the IM of Fig. 1.

$$R_\mathrm{s}^{'} = R_\mathrm{s} \cdot \Big(1 + \alpha \left(\vartheta_\mathrm{sim,new} - \vartheta_\mathrm{ref}\right)\Big) \tag{1}$$

$$P_\mathrm{L,ohm,s}^{'} = 3 \cdot {I_\mathrm{s}}^2 \cdot R_\mathrm{s}^{'} \tag{2}$$

B. Temperature Scaling of the Rotor Resistance

In contrast to the stator resistance the rotor resistance R_r is defined in the preprocessing of the FE simulation in the form of a compensating conductivity as described in [7]. The temperature variation of the rotor cage and rotor conductivity respectively can be considered by the second rotor resistance scaling factor $\mathrm{k_{R2}}$ introduced in [7]. It is dependent on the old and new conductivity, σ_r and $\sigma_\mathrm{r,new}$, the old and new temperature coefficients α and α_new, the old and new reference temperatures ϑ_ref and $\vartheta_\mathrm{ref,new}$ and the old and new simulation temperatures ϑ_sim and $\vartheta_\mathrm{sim,new}$.

$$\mathrm{k_{R2}} = \frac{\sigma_\mathrm{r}}{\sigma_\mathrm{r,new}} \frac{1 + \alpha_\mathrm{new}\left(\vartheta_\mathrm{sim,new} - \vartheta_\mathrm{ref,new}\right)}{1 + \alpha\left(\vartheta_\mathrm{sim} - \vartheta_\mathrm{ref}\right)} \tag{3}$$

By neglecting the other scaling possibilities in [7], such as geometric scaling, the temperature change in the rotor cage yields the scaled rotor resistance:

$$R_\mathrm{r}^{'} = R_\mathrm{r} \cdot \mathrm{k_{R2}} \tag{4}$$

and to the scaled Ohmic losses of the rotor $P_\mathrm{L,ohm,r}^{'}$:

$$P_\mathrm{L,ohm,r}^{'} = P_\mathrm{L,ohm,r} \cdot \mathrm{k_{R2}}, \tag{5}$$

that are used in the thermal model of the IM of Fig. 1.

IV. Calculation of Induction Machines considering temperature changes

With the parametrized thermal three node model of the IM a continuous operation of the machine with a torque of $T = 56\,\mathrm{N\,m}$ and a speed of $n = 3700\,\mathrm{rpm}$ is simulated once without a rescaling of the Ohmic losses in the stator and rotor due to a temperature change and once with rescaling the Ohmic losses of the machine. The results in Fig. 2 show that the consideration of the temperature variations have a high influence on the thermal behavior of the IM. The simulation with scaled machine achieves a lower temperature in the first 1500 s and a much higher temperature after 1500 s.

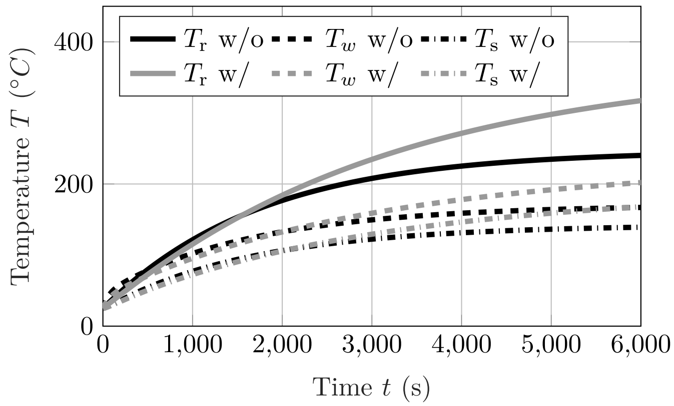

Figure 2: Results of the Temperature Simulation with (w/) and without (w/o) rescaling of the IM.

V. Conclusions and Further Work

In this paper a parametrized analytic thermal three node network model of an IM is proposed. Furthermore, the scaling laws of an IM are used to scale the FE solutions due to temperature variations in the stator and rotor of the machine. A thermal simulation with and without using the presented scaling approach shows a high influence on the simulated thermal behavior of the IM considering temperature scaled machine losses or not. The full paper will present more detailed descriptions of the thermal model, the scaling procedure and the influence of the temperature consideration in the thermal simulation. It will also emphasize the rapid calculation of the method.

References

[1] L. Alberti and N. Bianchi, "A coupled thermal–electromagnetic analysis for a rapid and accurate prediction of im performance," *IEEE Transactions on Industrial Electronics*, vol. 55, no. 10, pp. 3575–3582, Oct 2008.

[2] S. Mezani, N. Takorabet, and B. Laporte, "A combined electromagnetic and thermal analysis of induction motors," *IEEE Transactions on Magnetics*, vol. 41, no. 5, pp. 1572–1575, May 2005.

[3] J. Puranen and J. Pyrhonen, "Optimization of the loadability of an induction servomotor with a coupled electromagnetic-thermal model," in *International Symposium on Power Electronics, Electrical Drives, Automation and Motion, 2006. SPEEDAM 2006.*, May 2006, pp. 153–158.

[4] M. Nell, G. von Pfingsten, and K. Hameyer, "Rapid parameter identification and control of an induction machine," *COMPEL - The international journal for computation and mathematics in electrical and electronic engineering*, vol. 37, no. 5, pp. 1678–1688, 2018.

[5] J. Pyrhönen, T. Jokinen, and V. Hrabovcová, *Design of rotating electrical machines.* John Wiley & Sons, Ltd, 2008.

[6] VDI-Gesellschaft Verfahrenstechnik und Chemieingenieurwesen, *VDI Wärmeatlas.* Springer Vieweg, 2013.

[7] M. Nell, J. Lenz, and K. Hameyer, "Efficient numerical optimization of induction machines by scaled fe simulations," in *2018 XIII International Conference on Electrical Machines (ICEM)*, Sept 2018, pp. 198–204.